Journal of Chromatography A, 658 (1994) 361–370
Elsevier Science B.V., Amsterdam

CHROM. 25 649

Validation of a theoretical model for adsorption using cephalosporin C and polymeric reversed-phase resins

E. Firouztale'*

TosoHaas, 156 Keystone Drive, Montgomeryville, PA 18936 (USA)

J.J. Maikner, K.C. Deissler and P.G. Cartier

Rohm and Haas Company, Spring House, PA 19477 (USA)

ABSTRACT

In this study a dynamic "rate-based" mathematical model of a chromatographic column was solved numerically and validated by the ability to predict breakthrough behavior of cephalosporin C on columns of Amberchrom reversed-phase media. This model accounts for axial dispersion, liquid film mass transfer, pore diffusion coefficient and incorporates a Langmuir non-linear isotherm.

The equilibrium isotherm for this system was determined experimentally and shown to follow a Langmuir isotherm. Batch adsorption studies were also performed and used to estimate the value of the pore diffusion coefficient. The model and the parameter values were shown to predict accurately the breakthrough of cephalosporin C on columns of Amberchrom reversed-phase media under different conditions. The validated model was further utilized to study the impact of each system variable on dynamics of cephalosporin C loading onto the column.

INTRODUCTION

As the need for efficient and cost effective separation and purification of biomolecules at large scales increases, it becomes important to develop techniques and protocols for optimization and efficient scale-up of these separations. One approach is to develop mathematical models which, once validated, can be utilized to study systematically the effect of each variable on the effectiveness of the purification.

Various mathematical models have been described in the past. The simpler models [1–4] assume a linear isotherm in order to obtain an analytical solution. These models are easy to use, however, they lack accuracy at overload conditions. The more complete models [5–7] which account for liquid film mass transfer, pore diffusion and non-linear isotherms require numerical methods to solve the set of partial differential equations that describe the system and are more difficult to use. The models described in the literature vary in the degree to which they have been validated experimentally.

This study was concerned with numerical solution and validation of a "rate-based" model previously described by other investigators [5,7]. Independent isotherm and batch adsorption studies, as described previously [8], were combined with non-linear regression to determine the key parameters of this model. The model and the key parameter values were validated by their ability to "predict" the breakthrough of cephalosporin C on columns of Amberchrom reversed-phase media under varying conditions. The validated model was further utilized to study the dynamics of loading of cephalosporin C as a function of resin size, column geometry and

* Corresponding author.

0021-9673/94/$07.00
SSDI 0021-9673(93)E1088-H

column operating variables. We hope that the study demonstrates the impact of the variables, individually and collectively, on the dynamics of the system.

THEORY

A theoretical model previously described by Cowan *et al.* [5] and Yamamoto [7] was used in this study. This model incorporates liquid film mass transfer, pore diffusion and axial dispersion. It also incorporates a non-linear isotherm.

The material balance for the mobile phase in the packed column is

$$\frac{\partial c}{\partial t} = D_a \frac{\partial^2 c}{\partial z^2} - u\frac{\partial c}{\partial z} - \frac{3}{R}\frac{V_S}{V_L} k_L (c - c_p)_{r=R} \quad (1)$$

where c is the concentration of the solute in the bulk fluid (mg/cm^3), c_p is the pore concentration of solute (mg/cm^3 pore volume), D_a is the dispersion coefficient (cm^2/s), R is the resin radius (cm), u is interstitial velocity (cm/s), V_L is the volume of the liquid phase (cm^3), V_S is the total volume of the adsorbent particles (cm^3), k_L is the liquid film mass transfer coefficient (cm/s), t is time(s) and r is the radial axis.

Assuming a pulse input, eqn. (1) is subject to the following initial and boundary conditions:

$$c(z, t = 0) = 0 \quad (2)$$

$$\text{at } z = 0, \quad 0 < t < t_0 \quad c = c_f$$

$$t > t_0 \quad c = 0 \quad (3)$$

$$\text{at } z = L, \quad \frac{\partial c}{\partial z} = 0 \quad (4)$$

where c_f is the feed concentration, t_0 is the duration of the pulse, z is the axis along the column length and L is column length (cm).

For the stirred tank which is utilized in the batch adsorption studies:

$$\frac{\partial c}{\partial t} = \frac{-3}{R}\frac{V_S}{V_L} k_L (c - c_p)_{r=R} \quad (5)$$

Eqn. 5 is subject to the initial condition

$$c(t = 0) = c_i \quad (6)$$

where c_i is the initial concentration of solute in the solution.

Material balance is applied to the adsorbent as well. The resulting equation for the adsorbent pore phase is:

$$\frac{\partial c_p}{\partial t} = D_p \left(\frac{\partial^2 c_p}{\partial r^2} + \frac{2}{r}\frac{\partial c_p}{\partial r}\right) - \frac{(1 - \epsilon_p)}{\epsilon_p}\frac{\partial q_p}{\partial t} \quad (7)$$

Here, D_p is the effective pore diffusion coefficient of the solute in the particle (cm^2/s), ϵ_p is the intraparticle void fraction and q_p is the solid phase concentration of solute (mg/cm^3 solid phase).

This equation is subject to two boundary conditions. The boundary condition at the surface of the resin is

$$\left(\frac{\partial c_p}{\partial r}\right)_{r=R} = \frac{k_L}{D_p \epsilon_p}(c - c_p)_{r=R} \quad (8)$$

The boundary condition to satisfy symmetry conditions is

$$\left(\frac{\partial c_p}{\partial r}\right)_{r=0} = 0 \quad (9)$$

It should be mentioned that the model equations for the adsorbent are applicable to both stirred tank and column models.

For the column model, additional equations are needed to describe the liquid film mass transfer coefficient (k_L) and the axial dispersion coefficient (D_a). For the liquid film mass transfer coefficient (k_L), the correlation of Arnold *et al.* [9] was utilized:

$$N_{Sh} = 2 + 1.45\, N_{Re}^{1/2}\, N_{Sc}^{1/3} = \frac{2\, k_L\, R}{D_f} \quad (10)$$

where

$$N_{Re} = \frac{2v\,\rho\,R}{\mu} \quad (11)$$

and

$$N_{Sc} = \frac{\mu}{\rho\, D_f} \quad (12)$$

N_{Re}, N_{Sc} and S_{Sh} are dimensionless Reynolds, Schmidt and Sherwood numbers, respectively; v is the open column velocity (cm/s), D_f is the bulk diffusion coefficient of the biomolecule (cm^2/s) and ρ(g/cm^3) and μ(g/cm·s) are den-

sity and viscosity of the mobile phase, respectively.

The empirical correlation of Gunn and Athalaye *et al.* [10–12] was utilized to represent the axial dispersion coefficient D_a:

$$\frac{1}{N_{Pe}} = \left\{ Z(1-p)^2 + Z^2 p(1-p)^3 \times \left[\exp\left(\frac{-1}{Z_p(1-p)} \right)^{-1} \right] + \frac{\epsilon_b}{1.4\, N_{Re}\, N_{Sc}} \right\} = \frac{2\, u\, R}{D_a} \quad (13)$$

where

$$p = 0.17 + 0.33 \exp\left(\frac{-24}{N_{Re}} \right) = \text{Packing Number} \quad (14)$$

$$Z = \frac{N_{Re}\, N_{Sc}}{9.62(1-\epsilon_b)} \quad (15)$$

and ϵ_b is the column void fraction. Note that in the axial dispersion coefficient equations, N_{Re} is based on interstitial velocity.

In the above model it is assumed that the rate of adsorption to the surface is fast compared to the rate of diffusion. As a result, the model assumes that the concentration on the surface can be related to the pore concentration by an equilibrium isotherm. As will be shown in the following sections, the adsorption of cephalosporin C onto the Amberlite XAD-16, XAD-1600 and Amberchrom CG-161 media follows a Langmuir isotherm. This isotherm has the following form:

$$q_p = \frac{Q_{max}\, c_p}{c_p + K_d} \quad (16)$$

where Q_{max} is the maximum capacity of the resin and K_d is the Langmuir isotherm equilibrium constant.

NUMERICAL TECHNIQUES

The model equations are in the form of partial differential equations. These equations were reduced to ordinary differential equations by the method of orthogonal collocation. For the adsorbent equation, the roots of an nth order Jacobi polynomial [13] were used as collocation points. We discovered that at least two internal collocation points are needed for numerical stability. Two additional collocation points, corresponding to the two boundary conditions, were also needed. For the column model equations, the roots of the Legendre polynomial [14] were used as collocation points. At least 30 internal collocation points were needed for numerical stability. Two additional collocation points, corresponding to column entrance and exit, were also used.

The resulting set of ordinary differential equations were solved by a variety of numerical methods on an IBM Risc workstation. In particular, the methods of Adams, Molton, Gear, Runge-Kutta-Fehlberg (3rd order and 5th order) were tested [15]. The method of Runge-Kutta-Fehlberg (5th order) was chosen for integration of column and adsorbent equations. A search method similar to the method of Nedler and Mead [16] was used to perform non-linear regression.

EXPERIMENTAL

Chemicals

Amberlite® XAD®-16 adsorbent and the 300 μm developmental XAD-1600 resin were obtained from Rohm and Haas (Philadelphia, PA, USA). Amberchrom® CG-161 resins were obtained from TosoHaas (Montgomeryville, PA, USA). All the resins are macroporous, styrenic, reversed-phase type resins with a surface area of approximately 900 m^2/g and porosity of 0.67 ml/ml. The resins are produced in a series of different average particle diameters, ranging from 35 to 600 μm. The specific particle diameter is listed in the text whenever appropriate.

The trifluoroacetic acid (TFA) and the potassium salt of cephalosporin C were obtained from Sigma Chemical Company (St. Louis, MO, USA). HPLC grade solvents and ACS reagent grade buffers and acids were obtained from Fisher Scientific (Fairlawn, NJ, USA).

Columns

A 15 × 0.46 cm I.D. PLRP-S 100 Å (Polymer Labs, Foster City, CA, USA) packed with 8-μm particles was used to analyze the fractions collected in the column runs. 10 × 1.0 cm I.D. glass columns obtained from Omnifit (Atlantic Beach, New York, USA) and 25 × 2.2 cm I.D. glass, adjustable length columns from Amicon (Beverly, MA, USA) were packed according to the resin manufacturers' recommendations [17]. Bed length was 6.2 cm for the Omnifit and 12.5 cm for the Amicon columns.

Apparatus

The isotherm and batch adsorption studies were analyzed on a Perkin-Elmer (Norwalk, CT, USA) Model Lambda 3B UV spectrophotometer, at 259 nm.

A Rainin HP pump (Rainin Instruments, Woburn, MA, USA) with a 0.01 to 9.99 ml/min head was used for the cephalosporin C column breakthrough studies. Fractions were collected with a Gilson Model 201 fraction collector (Gilson, Middletown, WI, USA).

Fraction analysis was run on a series 4 liquid chromatograph equipped with an ISS-100 autoinjector with refrigerated sampling tray, a Kratos Model 783 UV detector (Perkin-Elmer). Data were handled by P.E. Nelson 2600 chromatography software, Rev. 5.10 (P.E. Nelson Systems, Cupertino, CA, USA).

Analytical chromatography conditions

Prior to analysis, fractions from the column runs were stored at 4°C to minimize cephalosporin C decomposition. Analysis was done in 8% acetonitrile–aqueous 0.1% TFA at 2.0 ml/min. Detection was at the λmaximum of cephalosporin C (259 μm). The injection size was 10 μl. Total analysis time was 10 min.

Preparation of cephalosporin C feed for column runs

The column loading experiments were run at pH 2.5 with a 3.5% sodium chloride background. The cephalosporin C potassium form was dissolved in water containing 3.5% sodium chloride at a concentration of 10 mg/ml and the solution was adjusted to pH 2.5 with concentrated sulfuric acid.

RESULTS AND DISCUSSION

Equilibrium isotherm studies

The equilibrium isotherms of cephalosporin C and four different size grades of resins were determined experimentally. For each resin, 50 ml of cephalosporin C solution, at the pH of 2.5, was mixed with 2 ml of moist resin. The concentrations of 0.1, 1.0, 2.5, 5.0, 10, 20, and 40 mg/ml were used for each isotherm study. The cephalosporin C solution and the resin were thoroughly mixed for 30 min by the action of an orbital shaker. The effluent was then withdrawn and its concentration determined by a UV spectrophotometer, at the wavelength of 259 nm, and after dilution.

The equilibrium isotherms for three different resins of the same chemical composition but having particle diameters of 84, 310 and 410 μm were determined and are shown in Fig. 1. The symbols are the experimental data and the solid line is the fit to the data, by non-linear regression, using a Langmuir isotherm. Note that all isotherms are practically identical. Therefore, as

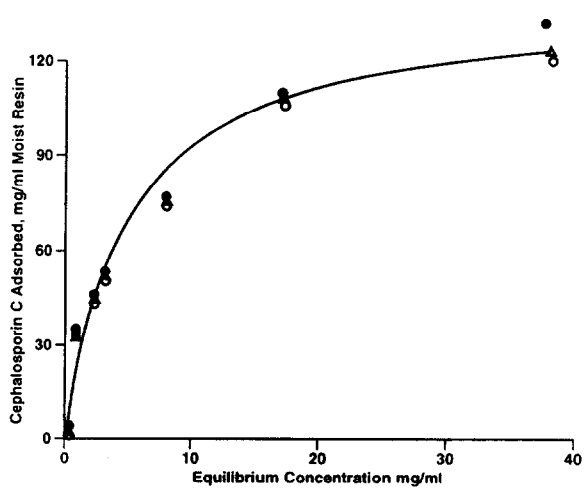

Fig. 1. Isotherms for three different particle diameters of XAD-16 type resins. The symbols are experimental results and the solid line is the fit to the data, by non-linear regression, obtained by a Langmuir isotherm. $Q_{max} = 132.0$ (± 5.5) mg/ml; $K_d = 4.88$ (± 0.63). Symbols: ● = 410 μm; △ = 310 μm; ○ = 84 μm.

theoretically acknowledged, these experiments prove that resins with similar chemical composition, surface area and porosity will have identical equilibrium isotherms. These results also indicate that in so far as cephalosporin C is concerned, the pore structure of all these resins is identical. The fit to the data also provides the maximum capacity of the resin at 132 mg/ml moist resin and the value of the Langmuir isotherm constant of 4.88 mg/ml. Therefore, isotherm studies define the shape of the isotherm and its key parameters.

Batch adsorption studies

To study the effect of particle size on the dynamics of adsorption of cephalosporin C by the resins, batch adsorption studies were performed. A 150-ml volume of cephalosporin C solution at a concentration of 11 mg/ml and pH of 2.5 was brought into contact with 6.4 ml of moist resin. The resin and the solution were thoroughly mixed using an agitator. At specific time intervals, small samples were withdrawn and their concentrations were determined by UV analysis at 259 nm as previously described.

In Fig. 2, the rate of adsorption of cephalosporin C by four different resin diameters is plotted against time. Note that the actual data are in the form of the drop in concentration as a function of time which can be easily converted to loading as a function of time. The rate of adsorption is faster for the smaller the particle size. Indeed, for the 84 μm diameter resin, the equilibrium is essentially reached by the time the first sample is withdrawn. The final (equilibrium) loading, however, is the same for all four grades consistent with the similarity of chemistry and surface area of the resins as evident by identical isotherms.

Fig. 3 is the same as Fig. 2 but with the X-axis normalized with respect to the square of the individual particle diameters. The four curves converge on a thin band with the curve for 84 μm being represented by a single point consistent with its flat profile. This normalization by the square of the diameter of the particle is consistent with the previous findings [8,18]. This normalization also indicates that, in addition to the surface area and chemical composition, the pore size distribution of the resins is the same, at least as far as cephalosporin C is concerned. It is, therefore, possible to use the square of the diameter to scale between various size grades. The specifics were described elsewhere [8].

Determination of the pore diffusion coefficient

Another key parameter is the effective pore diffusion coefficient (D_p). The model of the

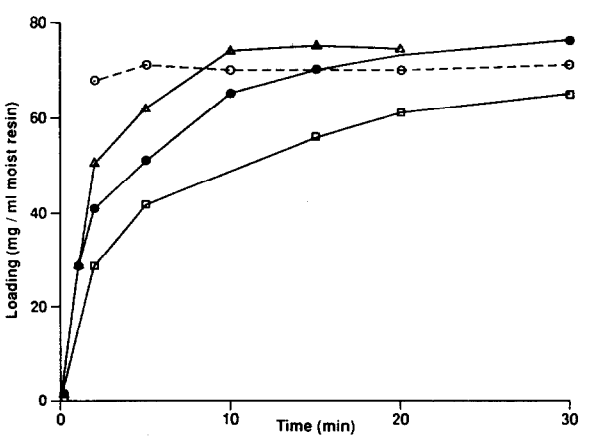

Fig. 2. The kinetics of uptake of cephalosporin C by three different size grades of Amberlite XAD-16 and Amberchrom CG-161md resin. Experimental data are depicted by symbols and connected by lines. Symbols: ● = 410 μm; △ = 310 μm; □ = 486 μm; ○ = 84 μm.

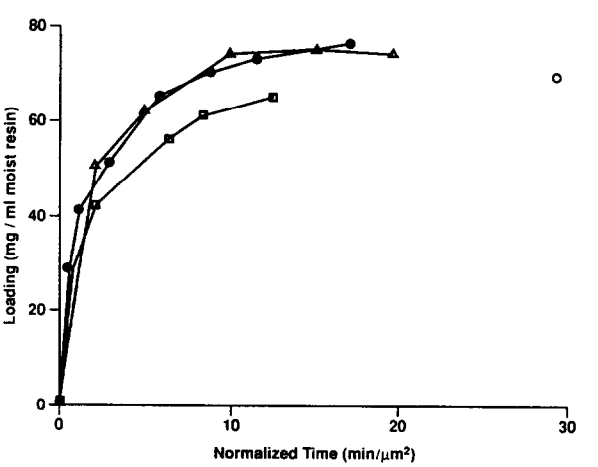

Fig. 3. Normalization of the kinetics of uptake of cephalosporin C. The X-axis of Fig. 2 is normalized with respect to square of the appropriate particle diameters. Lines and symbols as in Fig. 2.

stirred tank, the shape of the isotherm and the isotherm parameter values, were used to fit the batch uptake curves by non-linear regression. The value of pore diffusion coefficient (D_p) and the liquid film mass transfer coefficient (k_L) were adjusted to find a least-squares fit to the data. Note that the value of the liquid film mass transfer coefficient in a stirred tank is not the same as that encountered in the column operations.

In Figs. 4 and 5, we show the fit to the batch uptake data of cephalosporin C by resins with the particle diameters of 410 and 310 μm, respectively. The fit to the data in both cases is reasonable and the values of the pore diffusion coefficient of $2.00 \cdot 10^{-6}$ and $2.15 \cdot 10^{-6}$ cm^2/s are essentially the same.

Model validation

The critical test for the validity of a model is not its ability to "fit" a given condition. Rather, it is the ability of the model to "predict" a given set of conditions that constitute the true test of the validity of the model, its assumptions and the estimated parameter values. In order to test the validity of the model, the column model, together with the isotherm shape and parameter values, and the estimated value of the effective pore diffusion coefficient (D_p) were used to predict the breakthrough of cephalosporin C on columns of Amberchrom CG-161 resins.

In Fig. 6, we compare the "predictions" of the model with the experimental breakthrough of cephalosporin C on a 6.2 × 1.0 cm I.D. column packed with Amberchrom CG-161md resin and operated at 458 cm/h. The model, together with the estimated parameter values and without additional parameter estimation, predicts the

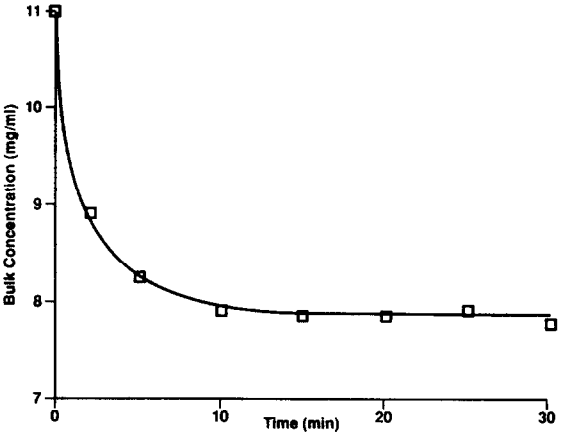

Fig. 5. Fit to the dynamic uptake studies of cephalosporin C by a XAD-1600 (310 μm). Symbols and line as in Fig. 4. The estimated pore diffusion coefficient has the value of $2.15 \cdot 10^{-6}$ cm^2/s.

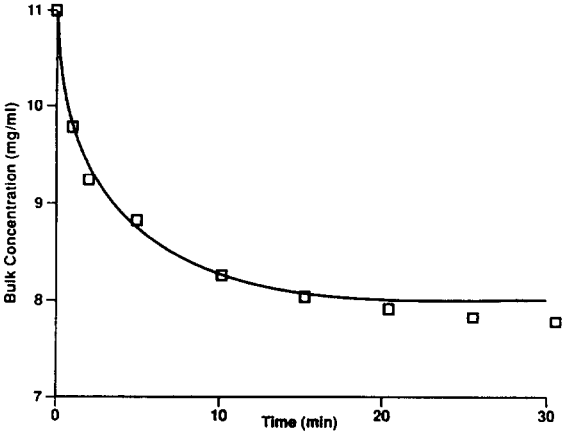

Fig. 4. Fit to the dynamic uptake studies of cephalosporin C by a 410 μm XAD-16 type resin. The symbols are experimental data and the solid line is the model fit to the data, by non-linear regression. The estimated pore diffusion coefficient has the value of $2.0 \cdot 10^{-6}$ cm^2/s.

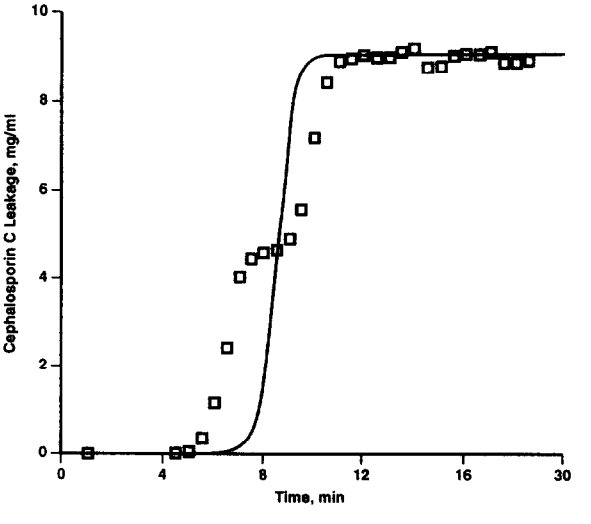

Fig. 6. Breakthrough of cephalosporin C on a 6.2 × 1.0 cm I.D. column packed with Amberchrom CG-161md resin (84 μm). Symbols and line as in Fig. 4. Open column velocity is 458 cm/h and feed concentration is 9 mg/ml.

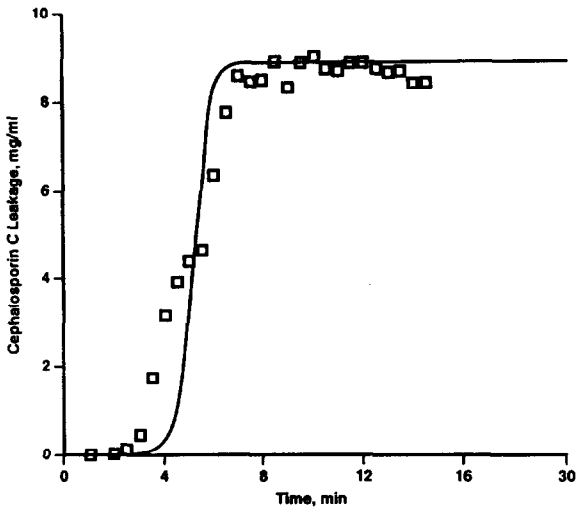

Fig. 7. Breakthrough of cephalosporin C on a 6.2 × 1.0 cm I.D. column packed with Amberchrom CG-161md resin (84 μm). Symbols and line as in Fig. 4. Open column velocity is 764 cm/h and feed concentration is 9 mg/ml.

breakthrough behavior well. In Fig. 7, we show a similar comparison for higher flow-rate of 764 cm/h. Again the model predictions and the experimental results are in good agreement indicating that the model represents the effects of flow rate well. In Fig. 8, the predictions of the model are compared with the experimental results for the larger particle diameter CG-161cd resin (115 μm). The model predicts the effects of the particle size as well.

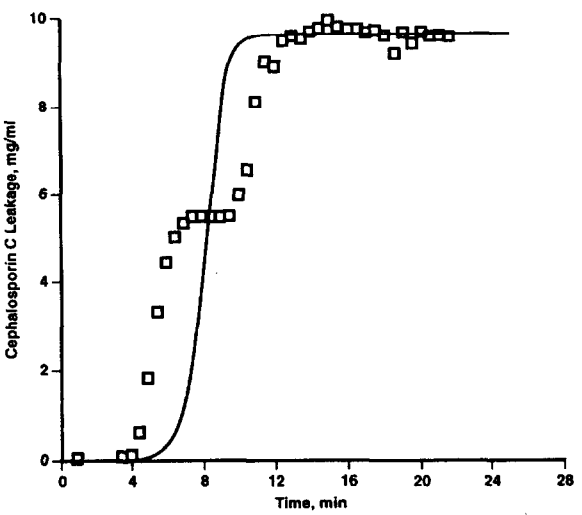

Fig. 8. Breakthrough of cephalosporin C on a 6.2 × 1.0 cm I.D. column packed with Amberchrom CG-161cd resin (115 μm). Symbols and line as in Fig. 4. Open column velocity is 458 cm/h. Feed concentration is approximately 10 mg/ml.

The experimental breakthrough curves in Figs. 6–8 show a characteristic displacement effect. This effect correlates with a pH shift in the column effluent which indicates that the initial breakthrough is a salt of cephalosporin C. This competitive adsorption is under study and will be the subject of another communication.

Simulations

The main advantage of a validated model is that it can be utilized to simulate experimental conditions. In this section, we utilize the model to analyze systematically the effect of particle size, flow rate and column length on adsorption performance. In this way, a validated model can be used as an effective tool for optimization and scale-up. These simulated values can be utilized, within the constraints of required production rates, acceptable pressure drops and acceptable resin cost (which increase as resin size decreases), to determine an optimum resin size for the given purification.

These simulations use flow rates, particle diameters and column lengths larger than those used to validate the model. The general nature of the model supports its use in this way. However, key simulations described in this section will be the subject of future experimental validation.

Effect of particle size

Fig. 9 depicts the effect of particle size on the breakthrough profile of cephalosporin C from a 12.5 × 2.0 cm I.D. column operated at 573 cm/h open column velocity. The curves correspond to particle diameters of 84, 116, 200, 310 and 486 μm. As expected, as the resin diameter decreases, the breakthrough profile becomes sharper and the time to breakthrough longer.

The results in Fig. 9 can be quantified by looking at the capacity at 1% breakthrough. Although there are other measures of column dynamics, we utilize the 1% breakthrough. This is defined as the loading onto the column at which the outlet concentration reaches 1% of the inlet concentration.

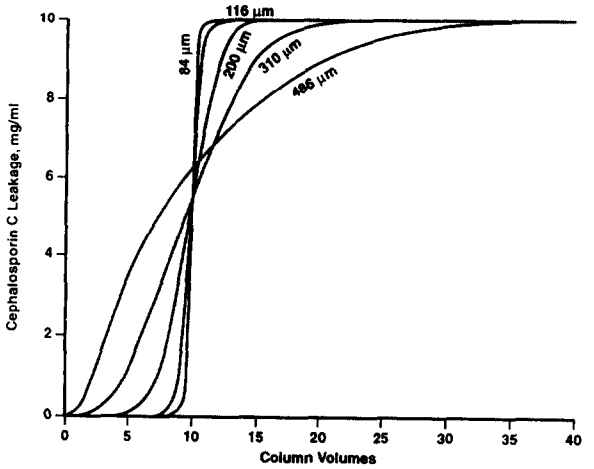

Fig. 9. Simulated effect of resin diameter on breakthrough of cephalosporin C. Feed concentration is 10 mg/ml, open column velocity is 573 cm/h in a 12.5 × 2.0 cm I.D. column. Resin diameters are indicated on the curves.

The simulations in Fig. 9 are tabulated in Table I in the form of key quantities: time to 1% breakthrough; dynamic capacity of the column at 1% breakthrough; and the efficiency. The efficiency is defined as the ratio of the dynamic capacity at 1% breakthrough to saturation dynamic capacity under the given conditions. The static capacity is the maximum isotherm capacity from Fig. 1. The pressure drop per m of the column was calculated by the Ergun equation [19].

The high adsorption efficiencies obtained for the 84 and 116 μm resins show that for cephalosporin C these small particles can be used in the relatively short 12.5 cm long bed. An increase in bed depth can offer little 1% dynamic capacity gain. The large particles show very low efficiency in this short bed. Either slower velocities or deeper beds can be used to optimize the performance of these particles.

Effect of bed depth

The dynamic capacity and, therefore, the column efficiency increase with an increase in column length. This is due to the fact that as the column length increases, the fraction of the column which is unsaturated when breakthrough occurs decreases.

Optimization of the 310 μm resin with respect to bed depth is shown in Table II. In the table, a 2 cm I.D. column packed with the 310 μm XAD-1600 resin is operated at 10 empty column volumes/h (573 cm/h). A six-fold increase in column length to 75 cm increases the capture efficiency from 0.24 to 0.80. An increase in bed depth above 75 cm will offer little 1% dynamic capacity gain. The high capture efficiency in the relatively short bed depth of 75 cm, combined

TABLE I

SIMULATED EFFECT OF RESIN DIAMETER ON LOADING OF CEPHALOSPORIN C ON COLUMNS OF XAD-16 TYPE RESIN

Column, 12.5 × 2.0 cm I.D.; velocity, 573 cm/h; feed concentration, 10 mg/ml.

Resin diameter (μm)	ΔP [a] (p.s.i./m)	Static capacity (mg/ml column)	Time to 1% leakage (min)	Dynamic capacity at 1% leakage (mg/ml column)	Efficiency [b]
84	34.4	132.0	11.57	73.0	0.89
116	18.4	132.0	10.42	65.8	0.80
200	6.4	132.0	6.49	40.9	0.51
310	2.4	132.0	3.02	19.0	0.24
486	0.8	132.0	1.07	6.7	0.08

[a] Calculated using the Ergun equation [19].
[b] Efficiency is defined as the ratio of the capacity at 1% leakage to total dynamic capacity.

TABLE II

SIMULATED EFFECT OF COLUMN LENGTH ON LOADING OF CEPHALOSPORIN C ON A COLUMN OF XAD-16 TYPE RESIN

Resin diameter, 310 μm; column internal diameter, 2 cm; velocity, 573 cm/h; feed concentration, 10 mg/ml.

Column length (cm)	ΔP [a] (p.s.i.)	Static capacity (mg/ml column)	Time to 1% leakage (min)	Dynamic capacity at 1% leakage (mg/ml column)	Efficiency [b]
12.5	0.32	132.0	3.02	23.0	0.24
25.0	0.66	132.0	11.88	45.3	0.46
50.0	1.27	132.0	35.97	68.7	0.70
75.0	1.90	132.0	61.60	78.4	0.80

[a] Calculated using the Ergun equation [19].
[b] Efficiency is defined as the ratio of the capacity at 1% leakage to total dynamic capacity.

with its pressure drop of about 2 p.s.i./bed (1 p.s.i. = 6894.76 Pa) make the 310 μm resin well suited for the adsorption of cephalosporin C.

Effect of velocity

The model can be utilized to examine the effect of velocity on column dynamics. Fig. 10 shows the breakthrough profiles for the 84 μm Amberchrom CG-161md resin in a 6.2 × 1.0 cm I.D. column. Sharp fronts are obtained even at

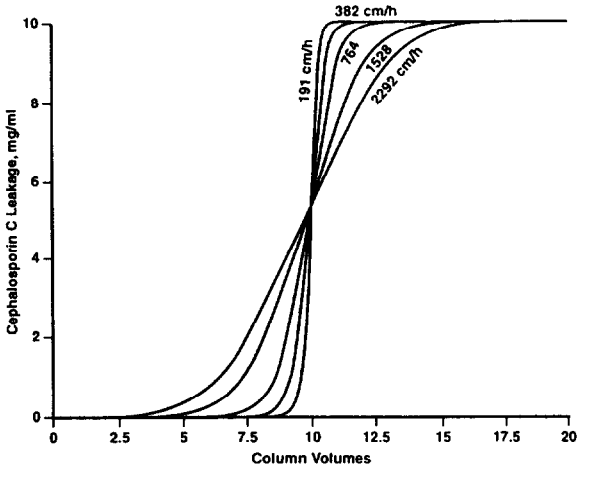

Fig. 10. Simulated effect of velocity on breakthrough of cephalosporin C. Feed concentration is 10 mg/ml, resin diameter is 84 μm and the column dimensions are 6.2 × 1.0 cm I.D. Velocities are indicated on the curves.

2300 cm/h with an efficiency of approximately 40%. The key quantities of the simulation in Fig. 10 are tabulated in Table III. These results demonstrate that these 84-μm particles offer high capture efficiency at high flows and in short columns. Of course, the pressure drop is higher than that experienced with the larger resins.

CONCLUSIONS

In this study, we have described a "rate-based" model of a chromatographic column. This model can be reduced to a stirred tank model as well which has utility for batch adsorption studies and for estimating pore diffusion coefficients. This model accounts for axial dispersion, liquid film mass transfer and pore diffusion. It incorporates a non-linear Langmuir isotherm and assumes that the rate of adsorption to the surface of the resin is fast compared to the rate of diffusion in the pores.

The model was solved numerically. Isotherms and batch adsorption studies were performed and utilized to obtain the key parameter values for the model independently. The model, its assumptions and the parameter values, were validated by the ability to predict, without additional parameter manipulation, the breakthrough profiles of cephalosporin C on columns packed with different diameter resins and operated

TABLE III

SIMULATED EFFECT OF VELOCITY ON LOADING OF CEPHALOSPORIN C ON A COLUMN OF AMBERCHROM CG-161M RESIN

Column, 6.2 × 1.0 cm; resin diameter, 84 μm; feed concentration, 10 mg/ml.

Velocity (cm/h)	ΔP [a] (p.s.i./m)	Static capacity (mg/ml column)	Time to 1% leakage (min)	Dynamic capacity at 1% leakage (mg/ml column)	Efficiency [b]
191	11.45	132.0	17.7	90.6	0.91
382	22.90	132.0	8.2	83.8	0.84
764	45.97	132.0	3.5	71.5	0.73
1528	92.26	132.0	1.3	52.2	0.53
2292	138.87	132.0	0.65	39.9	0.41

[a] Calculated using the Ergun equation [19].
[b] Efficiency is defined as the ratio of the capacity at 1% leakage to total dynamic capacity.

under different conditions. The validated model was then used to simulate the effect of resin diameter, velocity and column geometry on the column dynamics.

The model presented in this study requires only the estimated values of pore diffusion coefficient, shape and parameter values of the isotherm for the resin and molecule under study, to predict profiles under various operating conditions. The rest of the structure of the model does not have to be changed. This validated model, together with key experimental runs, can be a powerful tool in optimization and scale-up of a given purification.

ACKNOWLEDGEMENT

We would like to acknowledge the assistance of Dr. S. Dalvie in the initial stages of developing the numerical solutions.

REFERENCES

1 L. Lapidus and N.R. Amundson, *J. Phys. Chem.*, 56 (1952) 984.
2 A. Rasmuson, *AIChE J.*, 27 (1981) 1032.
3 S.J. Gibbs and E.N. Lightfoot, *Ind. Eng. Chem. Fundam.*, 25 (1986) 490.
4 J.T. Hsu and T.-L. Chen, *J. Chromatogr.*, 404 (1987) 1.
5 G.H. Cowan, I.S. Gosling J.F. Laws and W.P. Sweetenham, *J. Chromatogr.*, 363 (1986) 37.
6 N.L. Wang and Q. Yu, *Computers Chem. Eng.*, 13, 8 (1989) 915.
7 S. Yamamoto, K. Nakanishi and R. Matsuno, *Ion Exchange Chromatography of Proteins (Chromatographic Science Series*, Vol. 43), Marcel Dekker, New York, 1988, pp. 47–56.
8 E. Firouztale', A.P. Scott, S.K. Dalvie and G.M. Von Blohn, *New Developments in Bioseparation (AIChE Symposium Series*, Vol. 88, No. 290), American Institute of Chemical Engineers, New York, 1992, p. 25.
9 F.H. Arnold, H.W. Blanch and C.R. Wilke, *Chem. Eng. J.*, 30 (1985) B25.
10 D.J. Gunn, *Trans. Inst. Chem. Eng.*, 457 (1969) T351.
11 D.J. Gunn, *Chem. Eng. Sci.* 42 (1987) 363.
12 A.M. Athalye, S.J. Gibbs and E.N. Lightfoot, *J. Chromatogr.*, 589 (1992) 71–85.
13 J. Villadson and M.L. Michelson, *Solution of Differential Equation Models by Polynomial Approximations*, Prentice Hall, Englewood Cliffs, NJ, 1978.
14 B.A. Finlayson, *Nonlinear Analysis in Chemical Engineering*, McGraw Hill, NY, 1980.
15 *Simusolv/ACSL, Modelling and Simulation Software, Reference Guide*, Dow Chemical Company, Midland, MI, 1990.
16 J.A. Nedler and R.A. Mead, *Computer J.*, 7 (1965) 308.
17 *Instructions for Hydrating, Conditioning, Packing and Cleaning Amberchrom CG-71, CG-161, CG-300 and CG-1000 Resins*, Publication 27A11, TosoHaas, Montgomeryville, PA, USA, May 1993.
18 M.R. Ladisch, R.L. Hendrickson and E. Firouztale', *J. Chromatogr.*, 540 (1991) 85.
19 R.B. Bird, W.E. Stewart and E.N. Lightfoot, *Transport Phenomena*, John Wiley, New York, 1960, pp. 196–200.